Christian-Albrechts-Universität zu Kiel

Geographisches Institut

Effects of Climate-driven Variability in Atlantic Nutrient Supply on Primary Production in the German Bight

Submitted by:

Josephine Eismann
josephine.eismann@gmail.com

Eike Martin Schütt
eike.schuett@hereon.de

Ariane Tepass
ariane@tepass-net.de

Lecture: Ecosystem Modeling

Prof. Dr. Kai Wirtz

Wintersemester 2020/ 2021

20.04.2021

Abstract

The German Bight is a highly productive sea area. While the nutrients in the coastal zone mainly originate from anthropogenic emissions (i.e. riverine nutrient loads), nutrient concentrations in offshore waters are also governed by large-scale climate variations like the North Atlantic Oscillation (NAO). As a result of climate change, nutrient inflow from the North-East Atlantic into the North Sea will decrease. We present an approach to estimate the effect of three different nutrient concentration scenarios on primary production in the German Bight during the spring bloom with a relatively simple numerical modeling approach. The scenarios include a baseline (today's nutrient concentration), a 2100 mean scenario relating to an RCP 8.5 emission scenario and an extreme reduction scenario to account for the projected ranges of increased NAO variability after 2100. Parameter settings of our model were assessed in comparison to OC-CCI data. The modelled net primary productions for the three scenarios show high a high productivity along the coast and low values in western offshore parts as well as in the Elbe estuary. They reveal a general reduction for all nutrient inflow scenarios (-2.8 % and -10.8 % for mean and extreme scenario, respectively). Our results highlight the ability of our model to replicate current baseline chlorophyll patterns, but also show model weaknesses in overestimation in the northwestern part of the German Bight, which may be a result of our model forcing and the East Anglian Plume mapped there. In some nearshore areas, our modeling results show underestimations.

Table of content:

1. List of Symbols and Acronyms

Table 1 List of symbols and acronyms

Acronym or Symbol	Description	Unit
GB	German Bight	
PAR	Photosynthetically active radiation	[mol photons m^{-2} d^{-1}]
Chl	Chlorophyll (concentration)	[mg m^{-3}]
N_0	Nutrient concentration at the shore	[mmol m^{-3}]
H	Water depth	[m]
H_0	Half saturation depth of nutrients	[m]
$N(H)$	Depth dependent nutrient concentration	[mmol m^{-3}]
N_{offset}	Nutrient concentration in infinite deep waters	[mmol m^{-3}]
K_N	Nutrient limitation constant	[-]
K_{N0}	Scaling parameter	[-]
P	Gross primary production rate	[d^{-1}]
K_I	Half-saturation constant of gross primary production rate	[mol photons m^{-2} d^{-1}]
P_m	Maximum primary production rate	[d^{-1}]
I	Photosynthetically active radiation (PAR)	[mol photons m^{-2} d^{-1}]

I_0	PAR at the surface	[mol photons m^{-2} d^{-1}]
z	Depth	[m]
ϵ	Attenuation coefficient	[m^{-1}]
z_1	Saturation depth of primary production	[m]
dt	Time step in Euler forward integration	[d]
m	Mortality rate	[d^{-1}]
$\overline{PP_N}$	Average depth integrated net primary production	[gC m^{-2} d^{-1}]
τ	Duration of the model run	[d]
PP_{tot}	Total primary production	[gC d^{-1}]
σ	Surface area of a grid cell	[m^2]

2. Introduction

The German Bight (GB) is the south-eastern part of the North Sea (Figure 1). It is characterized by the transition of brackish waters in the estuaries to oceanic waters in the central North Sea with maximum water depths of around 70 m (Emeis et al., 2015).

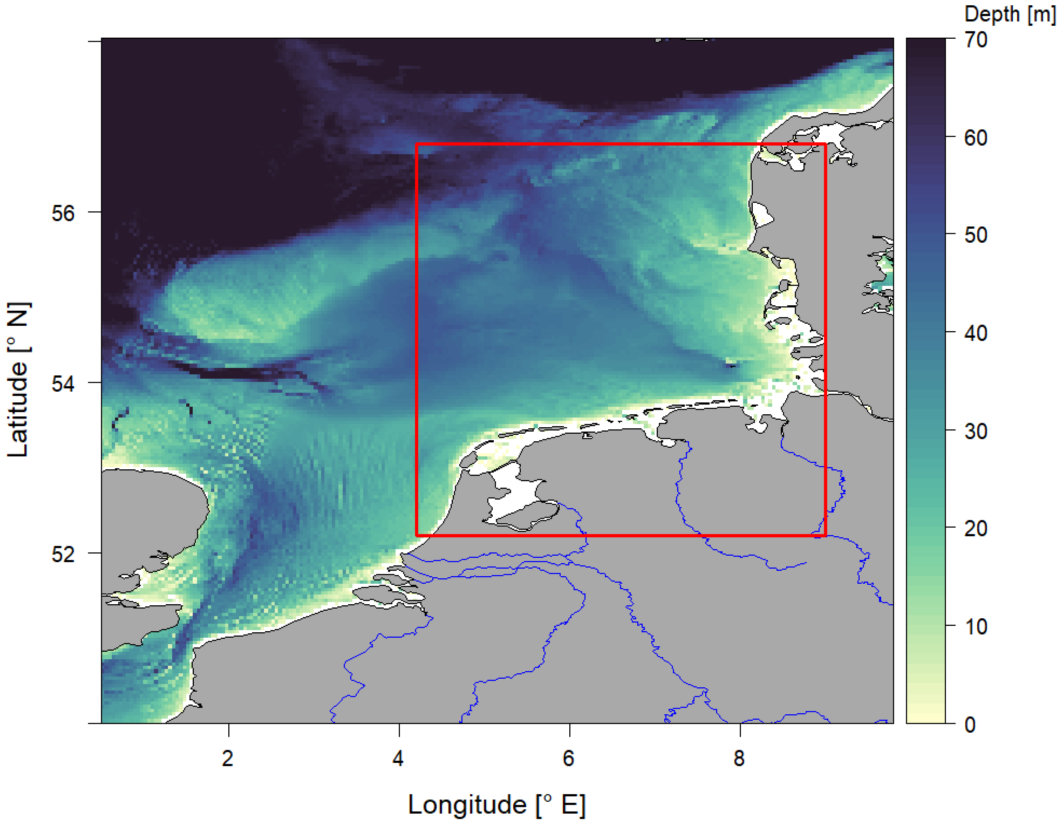

Figure 1: Bathymetric map of the southern North Sea. The red rectangle marks our study area.

As a consequence of relatively high nutrient inputs, mainly from rivers and the atmosphere, the GB is a highly productive sea area (Emeis et al., 2015). It has shown signs of eutrophication like oxygen minima since the 1980s, although inputs of Nitrogen (N) and Phosphorus (P) through rivers have been reduced significantly after an agreement of all riparian countries in 1987 (Brockmann et al., 2018; Große et al., 2017). Today, the Marine Strategy Framework Directive (MSFD) of the European Union defines the political aim to achieve a “good environmental status” (Emeis et al., 2015).

Nutrient concentrations and primary production are not evenly distributed in the GB. In fact, a strong coast-offshore gradient exists. Rivers still discharge considerable amounts of nutrients into coastal waters (Große et al., 2017). Their importance for the total nutrient budget decreases with increasing distance to the shore. In the offshore domain, nutrient concentrations are much smaller and largely independent of river discharges (Emeis et al., 2015). Instead, inflow of nutrients with water from the North Atlantic contributes with 50 to 100 % to the N budget along the 50-m-isobath and the central North Sea, respectively (Große et al., 2017).

A similar coastal-offshore gradient can be found for primary production. Chlorophyll concentrations (Chl) reach a mean of > 10 mg m^{-3} along the coast, while most offshore areas are much less productive (< 1 mg m^{-3}) (Xu et al., 2020).

Nutrient inputs and thus primary production are not only governed by anthropogenic emissions, but also by large scale climate variations like the North Atlantic Oscillation (NAO) (Pätsch and Kühn, 2008). A high NAO for example is associated with stronger westerly winds, increasing the inflow of nutrient rich waters masses from the North-East Atlantic and thus allowing a higher primary production in offshore waters of the GB (Emeis et al., 2015). Several models agree that the nutrient inflow from the North-East Atlantic into the North Sea will decrease as a result of climate change (Mathis et al., 2019; Gröger et al., 2013). An increasing temperature and a freshening of the upper ocean in the Atlantic will lead to a shoaling of the ocean mixed layer depth, which will in turn limit the nutrient transport from intermediate depths to the euphotic zone. Mathis (2019) estimated that the reduction of nutrients will be less severe in the North Sea than previously suggested, because mixing along the shelf break also contributes to the import of nutrients from the intermediate depths of the ocean into the shallow North Sea. The inflow of Atlantic PO_4 (the limiting element in offshore waters) into the Southern North Sea could reduce by ~24 % under an RCP8.5 emission scenario. Additionally, the interannual and decadal variability may increase considerably in the far future (i.e. after 2100).

The reduction of Atlantic nutrient inflow and its enhanced variability will likely also affect the primary production in the offshore part of the GB. Impacts on primary production will in turn have effects on higher trophic levels and thus also on economically relevant fish stocks and the fishery industry (Capuzzo et al., 2018). It may also impact the uptake of atmospheric CO_2 (Mathis et al., 2019; Emeis et al., 2015). Thus, a strong need to quantify possible impacts of changes in Atlantic inflow on primary production emerge.

In this paper we will estimate the primary production in the GB during a spring bloom for three different nutrient concentration scenarios using a relatively simple numerical modeling approach. The scenarios include a baseline (today's nutrient concentration), a scenario for the year 2100 under an RCP8.5 emission scenario and an extreme reduction scenario that accounts for enhanced NAO variability after 2100. We will first describe our model and scenarios in the section Methods before describing the Results. In the section Discussion we will compare the different scenarios and discuss the limitations of our modelling approach. Finally, we will summarize our main findings in the section Conclusions.

3. Methods

In this study, we develop a relatively simple numerical model for primary production in R (Version 4.0.3). Data and code are available in a GitHub repository (see section Data & Code availability).

3.1 Light limitation

In the GB, limiting factors for phytoplankton growth are mainly light and nutrient availability. In turbid, nutrient-enriched coastal waters, light availability limits phytoplankton growth (McQuatters-Gollop et al., 2007).

Light entering the water column is partly transmitted, scattered, or absorbed by the water itself and its constituents (Dörnhöfer and Oppelt, 2016). Hence, the photosynthetically active radiation (PAR) I decreases with depth z. This attenuation can be quantified as

$$I(z) = I_0 \cdot e^{-\epsilon z} \qquad [1]$$

where I_0 is the PAR at the surface, ϵ the attenuation coefficient and z the water depth. I_0 depends on the latitude and the Julian date and was estimated using a model provided by Kai Wirtz (pers. comm.) based on Campbell and Aarup (1989).

The gross primary production rate of phytoplankton P depends on the available light. This relationship can be described as a Michaelis-Menten function since the primary production rate in the dark ($I = 0$) is zero and converges towards a maximum primary production rate in bright conditions. The relationship can be approximated using the piecewise linear function

$$P = P_m \cdot \begin{cases} \dfrac{I}{2K_I} : if\ I < 2K_I \\ 1 : \qquad else \end{cases} \qquad [2]$$

with P_m as maximum primary production rate and K_I as half-saturation constant. This piecewise linear function assumes a linear increase of P with respect to I until P_m is reached at $2K_I$.

Zhao et al.(2019) showed that more than two-thirds of about 40,000 Chl profiles from the inner GB were vertically homogeneous and suggested that this proportion may in fact be even larger due to the relatively turbulent hydrodynamic conditions in the GB. For simplicity, we, therefore, assume that the water column in our model is perfectly mixed. Thus, we can combine equations [1] and [2] and calculate the integral average primary production $\bar{P}$ as

$$\bar{P} = P_m \epsilon^{-1} \cdot \left(\epsilon Z_1 + 1 - \frac{I(H)}{I(Z_1)}\right) \cdot \frac{1}{H} \qquad [3]$$

where Z_1 is the saturation depth of primary production (i.e. the deepest depth where the light allows maximum primary production rate), thus

$$I(z_1) = 2 * K_I \quad [4]$$

Combining this with Equation [1] and solving for z_1 yields

$$z1 = -\frac{1}{\epsilon} \cdot ln\left(\frac{2K_I}{I_0}\right) \quad [5]$$

3.2 Nutrient limitation

Nutrient concentrations sharply decrease with increasing distance to the shore. Xu et al. (2020) have shown that the distance to the shore can be approximated in the GB by water depth. The depth-dependent nutrient concentration $N(H)$ can be approximated by

$$N(H) = \left(N_0 - N_{offset}\right) \cdot \frac{H_0}{H_0 + H} + N_{offset} \quad [6]$$

where N_0 is the nutrient concentrations at the coast, H_0 is the half-saturation depth of nutrients and H is the water depth. The parameter N_{offset} defines the nutrient concentration the function converges to in deep waters. It is introduced to modify the offshore nutrient concentrations for different Atlantic inflow scenarios (see section Atlantic inflow scenarios).

The depth dependence in nutrient limitation has been defined as

$$f_N(H) = \frac{K_N}{K_{N0}} \cdot \frac{N(H)}{N(H) + K_N} \quad [7]$$

K_N denotes a unknown nutrient limitation constant and K_{N0} a scaling parameter.

3.3 Model forcing and parameter optimization

To predict Chl concentrations an Euler forward integration is used. Initial values for Chl and ϵ at a time t were taken from monthly averages of the 5th reprocessing of the Ocean-Colour Climate Change Initiative (OC-CCI) (Sathyendranath et al., 2019). The data is available on https://www.oceancolour.org/thredds/ncss/grid/CCI_ALL-v5.0-MONTHLY/dataset.html. Note that the OC-CCI products chlor_a and kd_490 were used for Chl and ϵ in this study. A bathymetry NetCDF-file (ESA CCI data) for the southern North Sea was provided by Kai Wirtz (pers. common).

We manually optimized our parameter settings by hindcasting the spring bloom in 2018. We forced our model with Chl from the OC-CCI monthly dataset of March and predicted in Chl in hourly time steps (i.e. $dt = \frac{1}{24}$) in order to minimize errors of our integration method. ϵ was initially also taken from OC-CCI data of March. After one month of prediction, the ϵ of the next month was used. This is necessary since our model does not account for changing turbidity (e.g. due to phytoplankton growth or sediment resuspension) itself.

The net growth rate (i.e. the change) depends on the nutrient concentration and light limitation, the mortality, and the standing stock of Chl:

$$ngr_t = Chl_t \cdot ((N(H) \cdot \bar{P}) - m) \quad [8]$$

Chl concentrations at time $t + dt$ were predicted based on the standing stock, the growth rate, and the length of time step dt:

$$Chl_{t+dt} = Chl_t + ngr_t \cdot dt \quad [9]$$

The prediction period was from March until May. Next, we compared our model result with the OC-CCI Chl data of May using a difference plot and iteratively optimized our parameter settings. The optimal settings and the corresponding difference plot are shown in section Results.

3.4 Atlantic inflow scenarios

Mathis et al. (2019) estimated that the winter (March) surface PO_4 concentration at the Atlantic shelf break south of Ireland fluctuated around 0.85 mmol m^{-3} since 1960. Under an RCP8.5 emission scenario, this will likely reduce to 0.65 mmol m^{-3} in 2100 (~ -24 % to present values) and show an enhanced interannual variability as a result of enhanced and/or prolonged NAO anomalies in the long term (i.e. after 2100). Projected winter surface PO_4 concentrations range from 0.25 mmol m^{-3} to present-day values (-70 % to 0%).

The reduction of Atlantic inflow will be less strong and less variable for weaker emission scenarios. We therefore assume, that the range of likely inflow scenarios is covered when comparing present-day inflow (baseline) to a reduction of -24 % (mean scenario) and -70 % as a not unrealistic extreme event.

The contribution of the Atlantic inflow to the nutrient budget increases with distance to the shore. At the north and northwestern end of our study area, it contributes with > 70 %, while atmospheric and riverine inputs are less important (Große et al., 2017). For simplicity, we assume that at a depth of 70 m (approximately the deepest depth in our study area), the Atlantic inflow is the only contributor to the nutrient budget. Our three different inflow scenarios are initialized by adjusting the N_{offset} parameter in Eq. [6] in a way that the nutrient concentration at a depth of 70 m is reduced by 0 %, 24 %, and 70 % compared to the original $N(H)$-function for the spring bloom 2018 (see section Results). We assume that no other parameters will change (e.g. no changes of riverine and atmospheric nutrient inputs or phytoplankton productivity/species distribution).

3.5 Scenario evaluation

The impact of the different Atlantic inflow scenarios was analyzed by calculating the average depth-integrated net primary production $\overline{PP_N}$. First,

$$\overline{PP_N} = \frac{1}{\tau}\sum_{t=t_0}^{t_n} C\,C \cdot ngr_t \cdot dt \cdot H \qquad [10]$$

where τ is the duration of the model run (in days) and CC is the C:Chl ratio. This is required to derive phytoplankton carbon estimates from the Chl concentrations. Based on Llewellyn (2004) we used $CC = 25$. Spatial characteristics of $\overline{PP_N}$ for the different scenarios were assessed by difference plots.

Finally, the total primary production of the GB PP_{tot} is calculated to quantify the differences in primary production across the whole region. PP_{tot} is equivalent to the sum of $\overline{PP_N}$ for each pixel p multiplied by the area of the respective pixel σ:

$$PP_{tot} = \sum_{i=1}^{p} \overline{PP_{N_i}} \cdot \sigma_i \qquad [11]$$

Each pixel of the OC-CCI raster has a size of ~ 0.0416 ° in both latitude and longitude direction. This means that σ of each pixel (measured in m²) decreases towards the north. To account for these differences (~ 12 % between pixels at the southern and northern boundary), σ is calculated for each row of the raster with the *areaPolygon*-function from the R-package *geosphere* (Karney, 2013).

4. Results

4.1 Parameter settings and Chlorophyll prediction

As discussed in the chapter Model forcing and parameter optimization, the different model parameters were manually optimized by hindcasting the period March - May 2018. For the baseline model, the following parameters were chosen:

$K_I = 15$, $m = 0.015$, $N_0 = 20$, $H_0 = 2$, $K_N = 1$, $K_{N0} = 5$, $N_{offset} = 2$

N_{offset} for the different nutrient inflow scenarios was chosen as described in Atlantic inflow scenarios (1.4 and 0.2 for the mean and the extreme scenario, respectively, see Figure A1).

A comparison of our model results and OCCCI Chl data for May 2018 (Figure **A**A2) shows a reasonable performance of the model in most parts of the GB. Generally, our model shows a clear coast-offshore gradient in Chl and predicted concentrations are close to the observations (mean absolute error 4.3 mg m^{-3}). The model shows the largest prediction errors in the Elbe estuary (underestimation), off Sylt and Rømø (overestimation) and in the north-west of our study area, where areas with low Chl concentrations is forecasted too far in the south.

4.2 Primary production for different scenarios

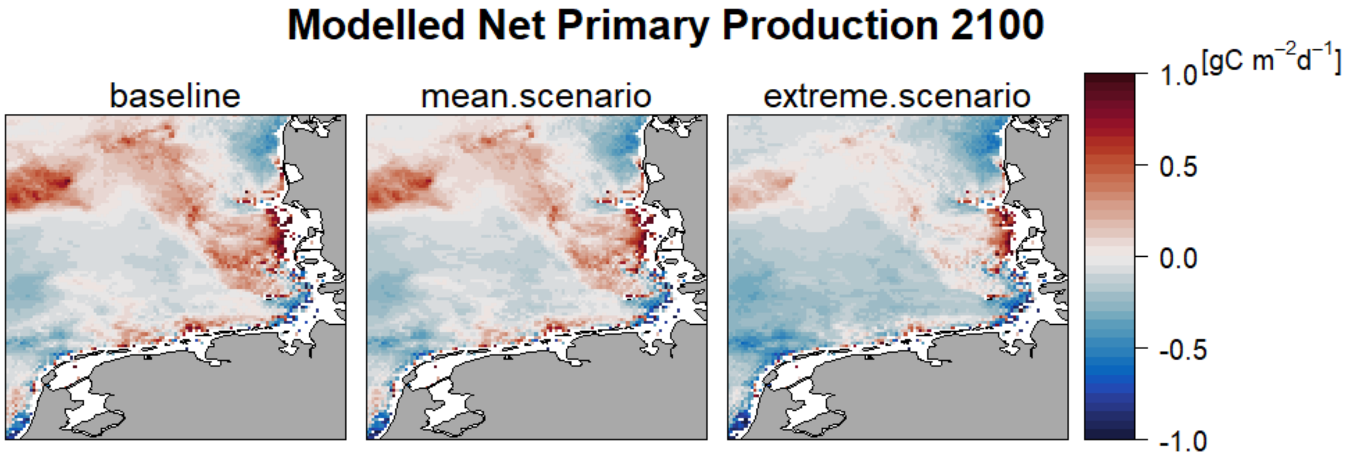

Figure 2 Net Primary Production in the German Bight modeled for a baseline scenario as well as the mean scenario and the extreme scenario.

Figure 2 presents the net primary production (NPP) for the baseline and the different nutrient inflow scenarios simulations. The baseline NPP is highest along most parts of the coast and slightly negative in the western offshore parts. Surprisingly, parts of the Elbe estuary have a low (negative) NPP. For the lower nutrient inflow scenarios, a reduction of NPP is visible. Overall, the NPP patterns are still similar to the baseline scenario, however, the reductions appear slightly more pronounced in the offshore domain.

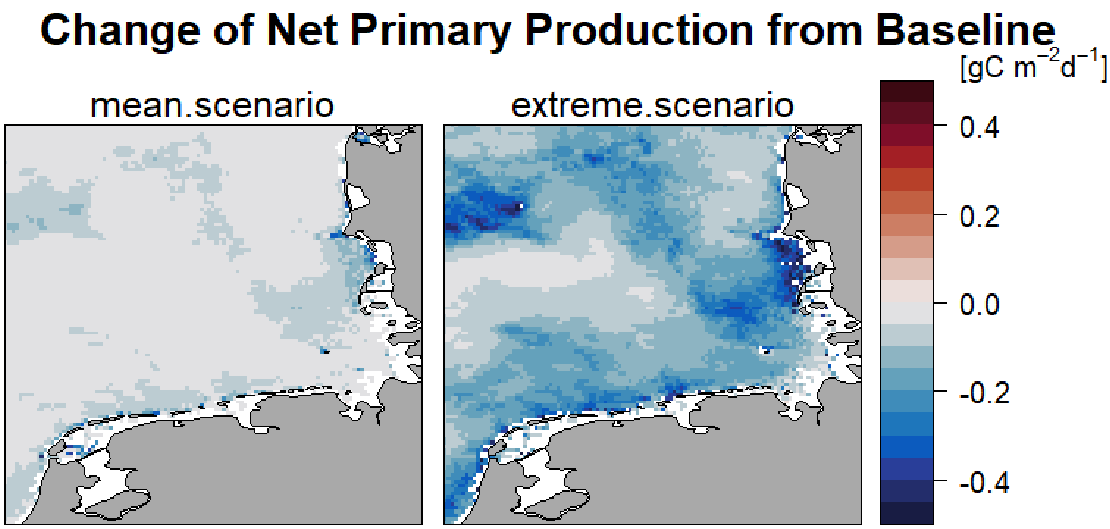

Figure 3 Differences between the net primary production of the mean and extreme scenario (2100) and the baseline (calculated as mean/extreme scenario – baseline).

As visible in Figure 3 the differences between the baseline and our mean scenario range between 0 and -0.2 gC m^{-2} d^{-1}; those between the baseline and under an extreme scenario are more pronounced and are mostly between -0.1 and -0.5 gC m^{-2} d^{-1}. Compared to the baseline, the spatially integrated NPP for the GB changes by -2.78 % and -10.79 % for the mean and the extreme scenario, respectively (Figure).

5. Discussion

5.1 Model consistency

Our hindcast of the spring bloom 2018 demonstrated the overall consistency of our model, as it reproduces fundamental patterns of Chl, like the coastal accumulation as a result of high nutrient availability and relatively low zooplankton grazing pressure (Wirtz, 2019). Looking at the differences between the model prediction and the ground truth data for May (Figure A2), the largest difference are Chl overestimations in the north-western part of the study area. OCCCI Chl data for March 2018 reveals that in this area Chl concentrations were elevated, likely as a result of the East Anglian Plume (Kwiatkowska et al., 2016). Our model predicted a positive primary production in this region, while the real Chl concentration decreased (see chapter Limitations for the reasons). However, directly south of this patch, the model predicts low Chl concentrations, which are typical for offshore waters (Xu et al., 2020).

The mean NPP calculated by our model for the baseline (519 gC m^{-2} yr^{-1}) exceeds observations (430 gC m^{-2} yr^{-1}, Rick et al., 2006) and ECOHAM model results (between 250 and 350 gC m^{-2} yr^{-1}, Emeis et al., 2015). It should be recalled that we model a spring bloom only. Phytoplankton growth is subject to strong seasonal patterns and usually peaks with a bloom between late Match and late April in the GB (Xu et al., 2020). During other times of the year, growth rates are considerably lower. Therefore, our NPP results appear to be within a reasonable range.

After the bloom, biomass remains high in the coastal zone, while it declines in transitional and offshore waters due to nutrient depletion and strong zooplankton grazing (Wirtz, 2019). Since we calculated NPP as the average NPP between March and May (slightly after the spring bloom), this pattern may explain negative NPPs in offshore waters (Figure 2).

5.2 Future Primary Production

Our nutrient inflow scenarios were based on model results from Mathis et al. (2019) and cover a wide range of likely future environmental conditions. It is expected that under an RCP8.5 emission scenario strong nutrient inflow variability may emerge after 2100 as a result of increased NAO variability. This variability spans from inflows similar to present-day inflows (baseline scenario) to a reduction of 70 % (extreme scenario), while an average reduction of -24 % is expected (mean scenario). Since we only cover inflows under an RCP8.5 emission scenario, we suggest that our mean and extreme scenarios are rather pessimistic. However, the range of the results of all three scenarios covers the range of realistic future nutrient inflow.

Figure 3 shows that a reduction of NPP may affect not only offshore, but also coastal regions in the GB. However, the impact on pelagic ecosystems will likely be larger than on coastal waters, because the relative NPP decrease is over proportionately large. Since in the entire North Sea phytoplankton primary production is at the base of marine food webs, this will have cascading effects across all higher trophic levels (Silberberger et al., 2018).

Our model does not include any stock assessments of higher trophic levels. However, analysis of declining primary production in the North Sea after ~1988 as a result of sea surface warming and reduced riverine nutrient input provide evidence that decreasing abundances of zooplankton and fish stocks may be expected in the future (Capuzzo et al., 2018). This would also negatively impact commercially important species and thus have knock-on effects on the fishery industry.

However, the effects of a reduced Atlantic nutrient inflow in the GB appears to be considerably smaller than in the northern North Sea (NNS), where nutrient concentrations are more dependent on Atlantic inflow and less on riverine inputs (McQuatters-Gollop et al., 2007). Modeling results project a NPP reduction of 21 % in the NNS for our mean scenario (Mathis et al., 2019) (compared to 2.78 % in the GB in our study). Nevertheless, changes of the ecosystems in the GB may occur, especially under our extreme scenario (NPP reduction of 10.78 %). We therefore highly encourage further studies to project possible ecosystem effects of a lower and more variable primary production.

5.3 Limitations

Despite our simple modeling approach, our model generates consistent results. However, apart from uncertainties that emerge from climate and nutrient inflow projections, the relatively simple structure of our model has some intrinsic limitations.

Our model did resolve the coastal accumulation, however, the estimates in the Elbe estuary were too low, while estimates along the North Frisian coast were too high (Figure **A**A2). We estimated nutrient concentrations as a function of depth, which is reasonable for most parts of the GB. However, in some areas like off the North Frisian coast (which is relatively shallow, see Figure 1) this simplification may not be accurate enough. We suggest that improvements in the coast-offshore gradient could be achieved by estimating nutrient concentrations from the salinity, which is an indicator for the contribution of riverine (nutrient-rich) and offshore (nutrient-poor) water (Mathis et al., 2019). To our knowledge, the mathematical relationship between salinity and nutrient concentration in the GB still needs to be determined, which should be done in further studies.

Another possibility to improve the coastal-offshore gradient would be to resolve zooplankton grazing dynamics more accurately. Phytoplankton grazing pressure is higher in the offshore domain than in coastal waters, because of an increase in carnivorous grazing in the coastal domain, where abundances of zooplankton predators (e.g. mussels or juvenile fishes) are higher (Wirtz, 2019). Including nutrient consumption of phytoplankton growth (and subsequent depletion) would also improve the coastal-offshore gradient (Mathis et al., 2019)

Additionally, the nutrient models for the different inflow scenarios (Figure A1) leave room for uncertainty. It is questionable, if the influence of Atlantic inflow at relatively low depths (i.e. 10-20 m) is as pronounced as in our model. To answer this question, more advanced biogeochemical modeling would be required, which was beyond the scope of this study.

Xu et al. (2020) have demonstrated that processes like de-eutrophication, changes in wind and temperature interact dynamically. Changes of the stressors may amplify or compensate each other and trigger unexpected system responses. For example, increasing water temperatures may allow a higher Phytoplankton productivity and thus mitigate lower nutrient inputs to some extend or alter species composition (Mathis et al., 2019; Emeis et al., 2015)

Considering all the limitations, our modeling approach may appear too simple to answer the question of how future NPP in the GB will change in the future and the results are certainly only rough estimates. However, it is a starting point to increase the understanding of the underlying ecosystem. The model also resolves the most fundamental processes of aquatic primary production and the hindcast of the spring bloom in 2018 demonstrates the applicability of the model. Still, further layers of complexity may be added to the model to improve its performance.

6. Conclusions

The presented numerical approach is able to model a clear coastal-offshore gradient in Chlorophyll concentration close to observations of OC-CCI data, with main prediction errors lying in the Elbe estuary, off Sylt and Rømø and in the northwestern part of the study area German Bight. The modeled baseline Net Primary Production shows the highest values along the coast, with negative parts in western offshore parts as well as in the Elbe estuary and map a general reduction of Net Primary Production for all nutrient inflow scenarios. Limitations of the developped model lie in the simplification of nutrient concentrations as a function of depth, which may not be sufficient for all regions of the German Bight, the lack of integration of grazing pressure as well as in uncertainties in the inflow scenarios and external ecosystem stressors.

7. Data & Code availability

Data and code of the model and the analysis and the results are available at https://github.com/eikeschuett/PhytoModGB.

8. References

Brockmann, U., Topcu, D., Schütt, M., & Leujak, W. (2018). Eutrophication assessment in the transit area german bight (north sea) 2006-2014 - stagnation and limitations. *Marine Pollution Bulletin*, *136*, 68–78. https://doi.org/10.1016/j.marpolbul.2018.08.060

Campbell, J. W., & Aarup, T. (1989). Photosynthetically available radiation at high latitudes. *Limnology and Oceanography*, *34*(8), 1490–1499. https://doi.org/10.4319/lo.1989.34.8.1490

Capuzzo, E., Lynam, C. P., Barry, J., Stephens, D., Forster, R. M., Greenwood, N., McQuatters-Gollop, A., Silva, T., van Leeuwen, S. M., & Engelhard, G. H. (2018). A decline in primary production in the north sea over 25 years, associated with reductions in zooplankton abundance and fish stock recruitment. *Global Change Biology*, *24*(1), e352–e364. https://doi.org/10.1111/gcb.13916

Dörnhöfer, K., & Oppelt, N. (2016). Remote sensing for lake research and monitoring – recent advances. *Ecological Indicators*, *64*(4), 105–122. https://doi.org/10.1016/j.ecolind.2015.12.009

Emeis, K.-C., van Beusekom, J., Callies, U., Ebinghaus, R., Kannen, A., Kraus, G., Kröncke, I., Lenhart, H., Lorkowski, I., Matthias, V., Möllmann, C., Pätsch, J., Scharfe, M., Thomas, H., Weisse, R., & Zorita, E. (2015). The north sea — a shelf sea in the anthropocene. *Journal of Marine Systems*, *141*(1556), 18–33. https://doi.org/10.1016/j.jmarsys.2014.03.012

Große, F., Kreus, M., Lenhart, H.-J., Pätsch, J., & Pohlmann, T. (2017). A novel modeling approach to quantify the influence of nitrogen inputs on the oxygen dynamics of the north sea. *Frontiers in Marine Science*, *4*, 287. https://doi.org/10.3389/fmars.2017.00383

Gröger, M., Maier-Reimer, E., Mikolajewicz, U., Moll, A., & Sein, D. (2013). NW european shelf under climate warming: Implications for open ocean – shelf exchange, primary production, and carbon absorption. *Biogeosciences*, *10*(6), 3767–3792. https://doi.org/10.5194/bg-10-3767-2013

Karney, C. F. F. (2013). Algorithms for geodesics. *Journal of Geodesy*, *87*(1), 43–55. https://doi.org/10.1007/s00190-012-0578-z

Kwiatkowska, E., Ruddick, K., Ramon, D., Vanhellemont, Q., Brockmann, C., Lebreton, C., & Hans, B. (2016). Ocean colour opportunities from meteosat second and third generation geostationary platforms. *Ocean Science*, *12*, 703–713. https://doi.org/10.5194/os-12-703-2016

Llewellyn, C. A. (2004). Phytoplankton community assemblage in the english channel: A comparison using chlorophyll a derived from hplc-chemtax and carbon derived from microscopy cell counts. *Journal of Plankton Research*, *27*(1), 103–119. https://doi.org/10.1093/plankt/fbh158

Mathis, M., Elizalde, A., & Mikolajewicz, U. (2019). The future regime of atlantic nutrient supply to the northwest european shelf. *Journal of Marine Systems*, *189*(3), 98–115. https://doi.org/10.1016/j.jmarsys.2018.10.002

McQuatters-Gollop, A., Raitsos, D. E., Edwards, M., Pradhan, Y., Mee, L. D., Lavender, S. J., & Attrill, M. J. (2007). A long-term chlorophyll dataset reveals regime shift in north sea phytoplankton biomass unconnected to nutrient levels. *Limnology and Oceanography*, *52*(2), 635–648. https://doi.org/10.4319/lo.2007.52.2.0635

Pätsch, J., & Kühn, W. (2008). Nitrogen and carbon cycling in the north sea and exchange with the north atlantic—a model study. Part i. Nitrogen budget and fluxes. *Continental Shelf Research*, *28*(6), 767–787. https://doi.org/10.1016/j.csr.2007.12.013

Rick, H. J., Rick, S., Tillmann, U., Brockmann, U., Gärtner, U., Dürselen, C., & Sündermann, J. (2006). Primary productivity in the german bight (1994–1996). *Estuaries and Coasts*, *29*(1), 4–23. https://doi.org/10.1007/BF02784695

Sathyendranath, S., Brewin, R. J. W., Brockmann, C., Brotas, V., Calton, B., Chuprin, A., Cipollini, P., Couto, A. B., Dingle, J., Doerffer, R., Donlon, C., Dowell, M., Farman, A., Grant, M., Groom, S., Horseman, A., Jackson, T., Krasemann, H., Lavender, S., … Platt, T. (2019). An ocean-colour time series for use in climate studies: The experience of the ocean-colour climate change initiative (oc-cci). *Sensors (Basel, Switzerland)*, *19*(19). https://doi.org/10.3390/s19194285

Silberberger, M. J., Renaud, P. E., Kröncke, I., & Reiss, H. (2018). Food-web structure in four locations along the european shelf indicates spatial differences in ecosystem functioning. *Frontiers in Marine Science*, *5*, 222. https://doi.org/10.3389/fmars.2018.00119

Wirtz, K. W. (2019). Physics or biology? Persistent chlorophyll accumulation in a shallow coastal sea explained by pathogens and carnivorous grazing. *PloS One*, *14*(2), e0212143. https://doi.org/10.1371/journal.pone.0212143

Xu, X., Lemmen, C., & Wirtz, K. W. (2020). Less nutrients but more phytoplankton: Long-term ecosystem dynamics of the southern north sea. *Frontiers in Marine Science*, *7*, 1205. https://doi.org/10.3389/fmars.2020.00662

Zhao, C., Maerz, J., Hofmeister, R., Röttgers, R., Wirtz, K., Riethmüller, R., & Schrum, C. (2019). Characterizing the vertical distribution of chlorophyll a in the german bight. *Continental Shelf Research*, *175*(19), 127–146. https://doi.org/10.1016/j.csr.2019.01.012

9. Appendix

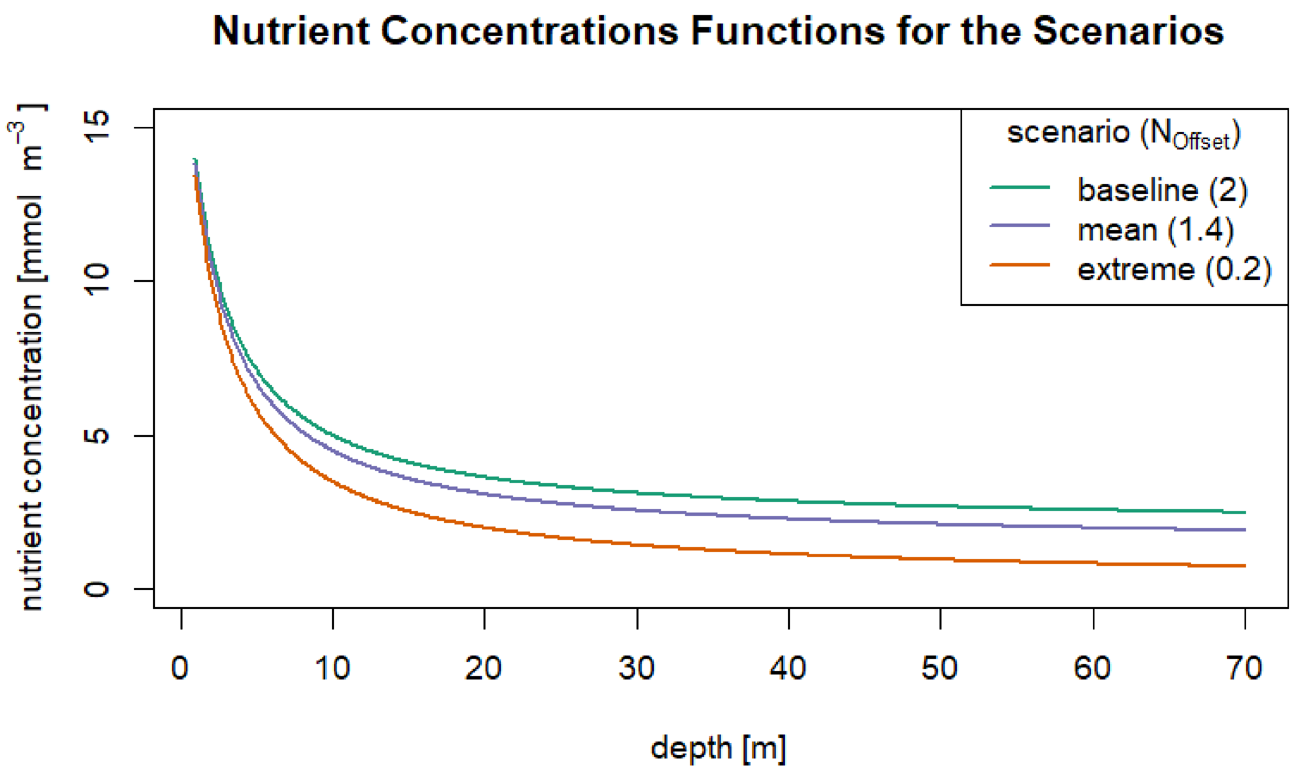

Figure A1: Depth-dependent nutrient concentration functions used for the different nutrient inflow scenarios.

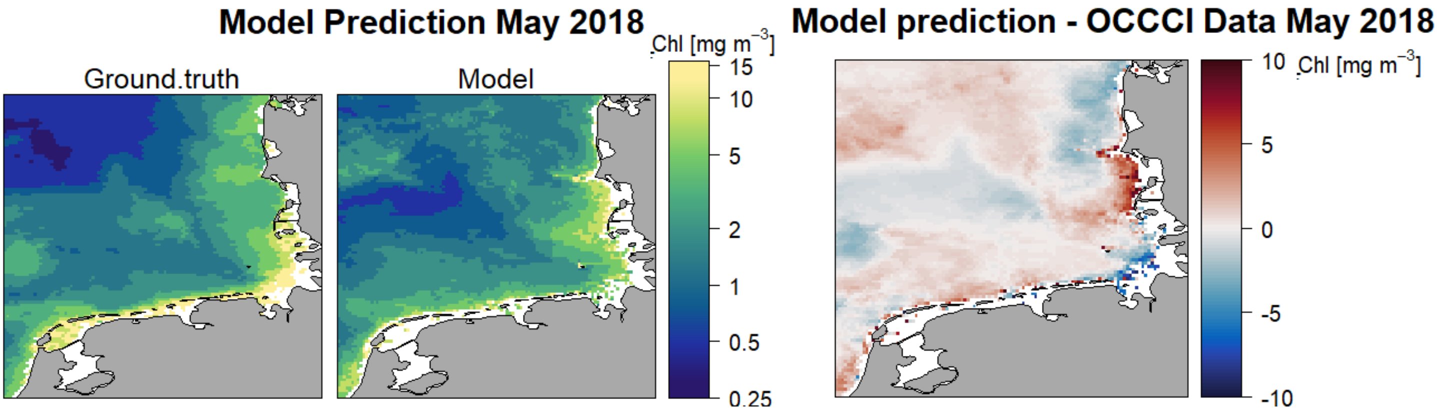

Figure A2*:* OCCCI ground truouth data, model result and difference plot of Chl model prediction and OCCCI Data for May 2018. The difference has been calculated as Model-OCCCI to evaluate the model quality.

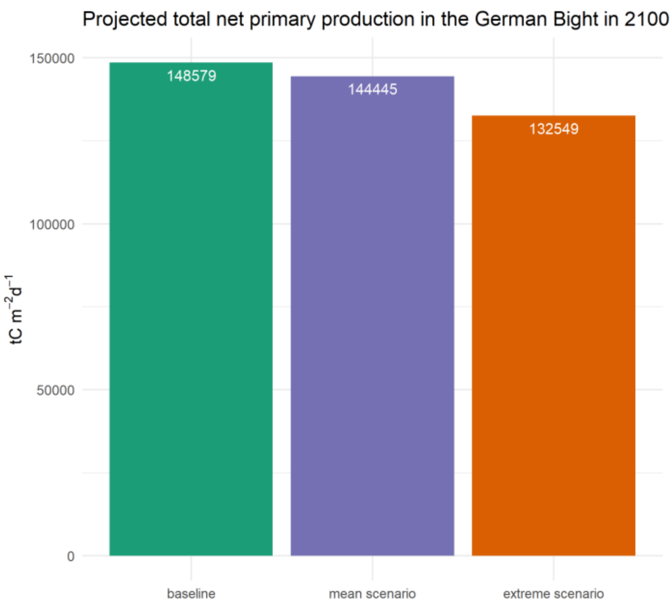

Figure A3*:* Projected spatially integrated total net primary production in the German Bight for the different scenarios.